

Coherent amplitudon generation in blue bronze through ultrafast interband quasi-particle decay

This article has been downloaded from IOPscience. Please scroll down to see the full text article.

2007 J. Phys.: Condens. Matter 19 346208

(<http://iopscience.iop.org/0953-8984/19/34/346208>)

View [the table of contents for this issue](#), or go to the [journal homepage](#) for more

Download details:

IP Address: 129.252.86.83

The article was downloaded on 29/05/2010 at 04:28

Please note that [terms and conditions apply](#).

Coherent amplitudon generation in blue bronze through ultrafast interband quasi-particle decay

Dodderi M Sagar^{1,3}, Artem A Tsvetkov¹, Daniele Fausti¹,
Sander van Smaalen² and Paul H M van Loosdrecht¹

¹ Zernike Institute for Advanced Materials, University of Groningen, 9747 AG Groningen, The Netherlands

² Laboratory of Crystallography, University of Bayreuth, 95440 Bayreuth, Germany

E-mail: p.h.m.van.loosdrecht@rug.nl

Received 28 March 2007, in final form 19 June 2007

Published 20 July 2007

Online at stacks.iop.org/JPhysCM/19/346208

Abstract

The charge density wave system $K_{0.3}MoO_3$ has been studied using variable pulse energy pump–probe spectroscopy, ellipsometry, and inelastic light scattering. The observed transient reflectivity response exhibits quite a complex behaviour, containing contributions due to quasi-particle excitations, coherent amplitudons and phonons, and heating effects. The generation of coherent amplitudons is discussed in terms of relaxation of photo-excited quasi-particles, and is found to be resonant with the interband plasmon frequency. Two additional coherent excitations observed in the transients are assigned to zone-folding modes of the charge density wave state.

(Some figures in this article are in colour only in the electronic version)

1. Introduction

A charge density wave transition is a metal to insulator transition originating from the inherent instability of a one-dimensional charge system coupled to a three-dimensional lattice [1–4]. Due to the electron–phonon coupling the electron density condenses in a charge-modulated state (modulation wavelength $\lambda = \pi/k_F$, with k_F the Fermi wavevector), and a charge density wave gap opens in the single-particle excitation spectrum at the Fermi energy. Above a certain temperature these materials are quasi-one-dimensional metals; below this temperature they are either insulators or semi-metals. Charge density wave systems exhibit a number of intriguing phenomena, ranging from Luttinger liquid-like behaviour in the metallic state [5] to highly nonlinear conduction and quasi-periodic conductance oscillations in the charge-ordered state [6, 4]. The nonlinear conduction seems to be a property which is not unique to charge density wave systems, as it is observed in other low-dimensional charge-ordering systems as

³ Present address: McGill University, Department of Chemistry, 801 Sherbrooke Street West, Montreal, QC, H3A 2K6, Canada.

well [7]. One of the well-known inorganic systems exhibiting charge density wave transitions is the blue bronzes [8]. The term bronze is applied to a variety of crystalline phases of the transition metal oxides. The bronzes with common formula $A_{0.3}\text{MoO}_3$, where the alkali metal A can be K, Rb, or Tl, are often referred to as *blue* bronzes because of their deep blue colour. The crystal structure of blue bronze contains rigid units comprised of clusters of ten distorted MoO_6 octahedra, sharing corners along the monoclinic *b*-axis [9]. This corner sharing provides an easy path for the conduction electrons along the $\langle 102 \rangle$ directions. The band filling is $3/4$ [3]. The particular material addressed in this paper is the quasi-one-dimensional metal $\text{K}_{0.3}\text{MoO}_3$, which undergoes the metal to insulator transition ($T_{\text{CDW}} = 183$ K) through the Peierls channel [9, 10].

Apart from the usual single-particle excitations (quasi-particles), charge density wave (CDW) systems possess two other fundamental excitations, which are of a collective nature. They arise from the modulation of the charge density $\rho(r) = \rho_0 + \rho_1 \cos(2k_{\text{F}}r + \phi)$, and are called phasons and amplitudons for collective phase (ϕ) and amplitude (ρ_1) oscillations, respectively. Ideally, the phason is a gapless Goldstone mode, leading to the notion of Fröhlich superconductivity [11]. However, due to the electrostatic interactions of the charges with the underlying lattice and possibly with impurities and imperfections, the translational symmetry of the state is broken, leading to a finite gap in the phason dispersion spectrum. In contrast, the amplitudon has an intrinsic gap in its excitation spectrum [12]. In centrosymmetric media the phason has a *ungerade* symmetry, and is therefore infrared active, and the amplitudon mode (AM) has a *gerade* symmetry and is hence Raman active [3, 13]. The phason mode is relatively well studied by, for instance, neutron scattering [14, 15] and far-infrared spectroscopy [3, 13], and plays an important role in the charge density wave transport. The amplitudon, i.e. the transverse oscillation of the coupled charge–lattice system, has been observed experimentally in, for instance, Raman experiments [9]. Ultrafast time-resolved pump–probe experiments have proved to be versatile tools in studies on the properties of CDW materials as well. Optically induced transient oscillatory conductivity experiments have shown that one can increase the coherence length of the CDW correlations by exciting quasi-particles from the CDW condensate [16]. An important breakthrough was the observation that one can coherently excite the amplitudon mode in pump–probe spectroscopy experiments [17–20]. These experiments open the possibility to study the temporal dynamics of the collective and single-particle charge density wave excitations, as well as their interactions with quasi-particles and vibrational excitations. Demsar *et al* [17] observed the amplitudon in $\text{K}_{0.3}\text{MoO}_3$ as a real-time coherent modulation of the transient reflectivity with the frequency of the amplitudon mode. The frequency and the decay time of the AM oscillation were measured as 1.67 THz and 10 ps, respectively. It was also found that the single-particle excitations across the CDW gap appear as a rapidly decaying (\sim ps) contribution to the transient reflectivity. The mechanism of the coherent AM generation was assumed to be displacive excitation of coherent phonons (DECP [21]), which is the mechanism which usually describes the generation of coherent phonons in absorbing media. The experiment was performed with the pump and the probe wavelength fixed at 800 nm and at a low pump power density of $1 \mu\text{J cm}^{-2}$. The aim of the present study is to obtain a better understanding of the transient response of the charge density wave material $\text{K}_{0.3}\text{MoO}_3$, and more in particular of the generation and dephasing mechanisms of coherent amplitudon oscillations. These issues are addressed using variable pump pulse energy pump–probe spectroscopy, ellipsometry and Raman scattering experiments.

2. Experimental details

A regenerative Ti:sapphire amplifier seeded by a mode-locked Ti:sapphire laser was used to generate laser pulses at 800 nm with a temporal width of 150 fs, operating at 1 kHz repetition

rate. The relatively low repetition rate minimizes heating effects due to the pile-up of the pulses, and all the experiments reported were performed with powers below the damaging threshold. To obtain laser pulses of continuously tunable energies, a travelling wave optical parametric amplifier of superfluorescence (TOPAS) was used. The output of the TOPAS is used as the pump pulse and the wavelength of the probe is kept at 800 nm throughout the experiment. The pump and the probe were each focused to a spot, of 100 and 50 μm diameter, respectively. In the wavelength-dependent measurements the pump pulse energy was kept constant (80 nJ/pulse), and in the pump pulse energy-dependent measurement the wavelength of the pump was kept constant (800 nm). The probe pulse energy was kept below 1 nJ/pulse. After experiments at high powers, the sample was checked for degradation by subsequently recording a low-power transient. No signs of degradation were observed during the experiments reported here. The polarization of the incident pump pulse was parallel to the b -axis along which the charge density wave ordering develops. The experiments were performed in a reflection geometry with the angle of the pump and probe pulses close to normal incidence with respect to the sample surface. The sample was placed in a He-flow cryostat, which allows one to vary the temperature between 4.2 and 300 K (stability ± 0.1 K). Raman experiments were performed using a microscope-equipped triple grating spectrometer, using 532 nm excitation (power density 500 W cm^{-2}). The ellipsometry experiments have been performed using a Woollam spectroscopic ellipsometer with the sample placed in a special home-built ultra-high vacuum (UHV) optical cryostat.

3. Transient reflectivity

The formation of the charge density wave in blue bronze leads to drastic changes in the nature of the transient reflectivity. This is exemplified in figure 1, which shows two representative transient reflectivity traces recorded above and below T_{CDW} obtained using 800 nm for both the pump and the probe wavelength. Above the phase transition ($T = 240$ K curve) the material is metallic and gapless, leading to a featureless very fast decay (faster than the time resolution, ~ 150 fs) of the excited electrons, followed by a slower decay which may be attributed to electron-phonon coupling induced heating effects. In the charge density wave state (figure 1 $T = 40$ K curve, and figure 2) the response is more interesting, due to the presence of various coherent excitations and a slowing down of the decay of the excited quasi-particles resulting from the opening of the CDW gap in the electronic excitation spectrum. A Fourier analysis of the response (see inset in figure 2) shows the presence of three coherent excitations. The strongest component found at 1.67 THz has been attributed to the coherent excitation of the collective amplitudon mode [17]. The two additional modes at 2.25 and 2.5 THz can be attributed to Raman-active phonons which are activated in the CDW state due to folding of the Brillouin zone [10]. Polarized frequency domain Raman scattering experiments have indeed confirmed this interpretation (see figure 3). The excitation wavelength for this experiment was 532 nm, with the polarization of the incoming and scattered light parallel to the b -axis of the crystal. Above the phase transition temperature ($T = 295$ K spectrum) the Raman spectrum is rather featureless in the region of the amplitudon mode. In contrast, the 2.7 K spectrum shows the appearance of just the three modes which are also observed in the time domain traces.

The observed transient reflectivity response in the CDW phase can be described by

$$\frac{\Delta R}{R} = A e^{-(t/\tau_{\text{QP}})^n} + \sum_j A_j e^{-t/\tau_j} \cos(\omega_j t) + B e^{-t/\tau_L}, \quad (1)$$

where the first term describes the quasi-particle response using a stretched exponential decay with time constant τ_{QP} and stretch index n , which takes the relaxation of the quasi-particles

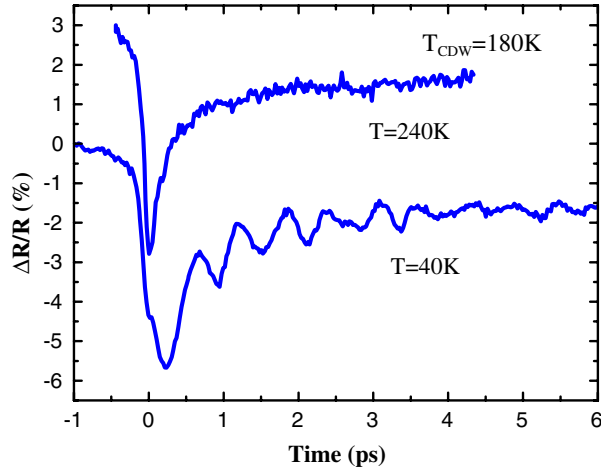


Figure 1. The transient reflectivity response of $K_{0.3}MoO_3$ above and below T_{CDW} . Transients are recorded using a wavelength of 800 nm for both pump and probe pulses, and a pump energy of 80 nJ/pulse. The 240 K transient has been given an offset for clarity.

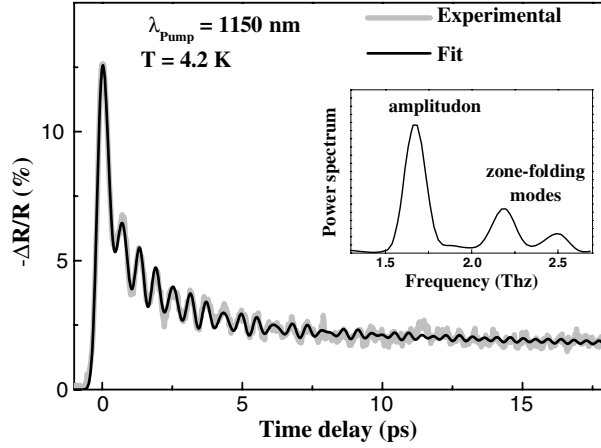


Figure 2. The transient reflectivity response of $K_{0.3}MoO_3$ at $T = 4.2$ K, using a 1150 nm pump pulse (80 nJ/pulse). The probe wavelength is 800 nm. The grey line represents a fit of equation (1) to the data. Inset: Fourier power spectrum showing the amplitudon mode at 1.67 THz, and two zone-folded phonons at 2.25 and 2.5 THz.

across the CDW gap into account. The second term in this expression accounts for the observed coherent amplitudon and phonon oscillations with frequencies ω_j and decay times τ_j , and the last term represents the observed long-time response with a decay time τ_L presumably originating from heating effects.

A fit of equation (1) to the data generally leads to excellent agreement with the data, as is for instance shown in figure 2. For this fit the quasi-particle decay time is found to be $\tau_{QP} = 0.65$ ps with $n = 1/2$, and the amplitudon lifetime $\tau_{AM} = 3.5$ ps. The decay times of the two coherent phonons is of the order of 20 ± 5 ps, whereas the cooling time is too slow to be determined with any accuracy ($\tau_L > 60$ ps). It is interesting to note that the coherent amplitudon is very short lived when compared to the two coherent phonons. This

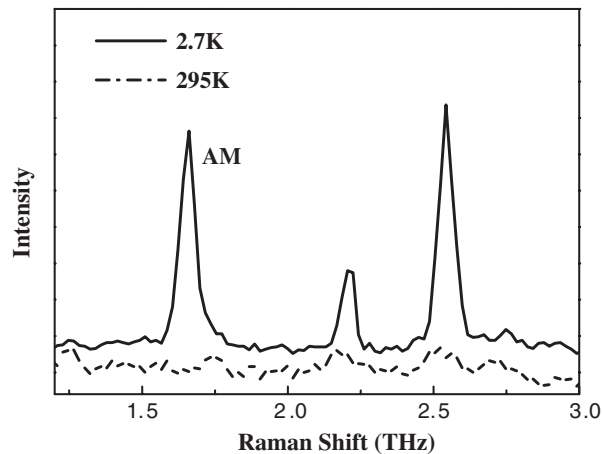


Figure 3. Polarized (bb) Raman spectra of $K_{0.3}MoO_3$ above and below the CDW transition temperature, showing the appearance of the amplitudon mode and the two fully symmetric modes.

heavy damping of the coherent amplitudon presumably results from amplitudon–quasi-particle scattering, leading either to a decay or to a dephasing of the coherent amplitudon excitation. The observation that the decay time in the present experiment is shorter than in the experiments by Demsar *et al* [17], who reported $\tau_{AM} = 10$ ps, is consistent with this. The density of excited quasi-particles in the current experiments is substantially higher (several orders of magnitude) than in the previous experiments, leading to this faster decay of the coherent amplitudon mode, and also to a larger magnitude of the induced response (here as large as 0.1, compared to 10^{-4} in [17]). The quasi-particle lifetime measured for the lowest pump power (0.1 mW, 8 nJ/pulse) is about 0.6 ps, which is close to the value measured by Demsar *et al* (0.5 ps) [17]. Besides the quasi-particle density, the main difference is that the experimental temperature in our case is $T = 4.2$ K, whereas in [17] it is $T = 45$ K. The stretched exponential behaviour observed in the present study, in contrast to the single exponent in Demsar’s study, might be due to the presence of a glassy state at low temperature which has recently been discussed in literature [22–24].

4. Pump pulse energy dependence

In order to address the generation mechanism of the coherent AM pump pulse energy-dependent (this section) and pump wavelength-dependent (see section 5) experiments were carried out. The experiments reported in figure 4 were performed up to a relatively high pump pulse energies (8–800 nJ/pulse, corresponding to 0.1–10 $mJ\ cm^{-2}$). Note that the data in figure 4 are scaled to the strength of the initial response, i.e. to the strength of the quasi-particle peak. The strength of the quasi-particle peak itself is found to be nearly linearly dependent on the pump pulse energy (see figure 5(b)); only at the highest energy (>300 nJ/pulse) does the response become sublinear. This linear dependence is consistent with the expectation that the density of the excited electrons scales with the number of photons in the pump pulse. If the generation mechanism of the coherent AM modes can be described, as suggested in [25], by the theory of displacive excitation (DECP) [21], one also expects a linear dependence of the amplitude of the coherent excitation with the pump pulse energy. In contrast, figures 4 and 5(a) clearly show that the relative intensity of the coherent amplitudon oscillations decreases dramatically with increasing pump pulse energy. This immediately rules

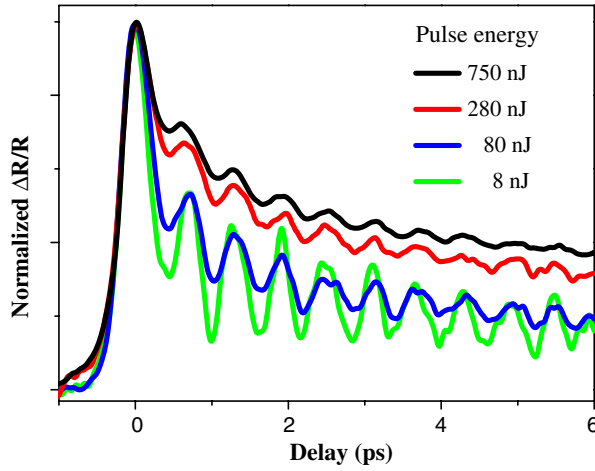


Figure 4. Normalized time-resolved reflectivity transients for 1150/800 nm pump-probe experiments with a pump energy ranging from 8 to 800 nJ/pulse (corresponding to 0.1–10 mJ cm⁻²). The data are normalized to the zero-delay response.

out the possibility of a linear relationship between the number of photons of the pump pulse and the observed amplitude of the coherent AM mode, and hence makes the pure DECP mechanism for the coherent amplitudon creation questionable. A second interesting feature of the pump pulse energy dependence of the time-resolved reflectivity transients is the substantial increase in the quasi-particle lifetime with the pump pulse energy (see figure 5(b)). Most likely, this increase occurs due to the presence of the CDW gap, which acts as a ‘bottle-neck’ in the relaxation process for the thermalized quasi-particles gas. The data suggest that the observed sublinear behaviour of the amplitudon generation might be correlated with increasing quasi-particle lifetime upon increasing pump pulse energy. Indeed, if the coherent amplitudons are not directly generated by a coupling to the photons, but rather by a coupling to the decay of the quasi-particle excitations, one would expect the observed behaviour provided that the initial phase of a substantial part of the amplitudons generated by the quasi-particle decay over the CDW gap is constant. That this is indeed the case is not obvious. Without any coherent amplification, one would normally expect that the phase of the generated amplitudon depends on the phase of the generating quasi-particle, which itself evolves rapidly in time, far more rapidly than the quasi-particle lifetime. In this phenomenological model, the increasing of the quasi-particle lifetime leads to a reduction of the coherence of the amplitudons generated, and thereby to a decrease in the amplitude of the coherent response. This results in a nearly full disappearance of the coherent amplitudon response once the inverse quasi-particle lifetime becomes of the order of the frequency of the amplitudon mode. In a crude and simple analytical approach, neglecting the temporal width of the pump pulse and the stretched exponential behaviour of the decay of the quasi-particle, one can model the quasi-particle response by a simple exponential decay ($e^{-t/\tau_{QP}}$ for $t > 0$), and a linear coupling between the quasi-particle decay and the amplitudon generation. The resulting coherent amplitudon response is then given by

$$I_{AM} = \int_0^{\infty} \frac{A}{\tau_{QP}} e^{-t'/\tau_{QP}} \cos(\Omega(t+t')) dt' = \frac{A}{1 + \Omega_{AM}^2 \tau_{QP}^2} \cos(\Omega t + \arctan(\Omega \tau_{QP})) \quad (2)$$

where A is the integrated area of the quasi-particle peak, Ω is the frequency of the AM, and τ_{QP} is the quasi-particle lifetime. The product $\Omega_{AM} \tau_{QP}$ plays the role of a coherence factor. For

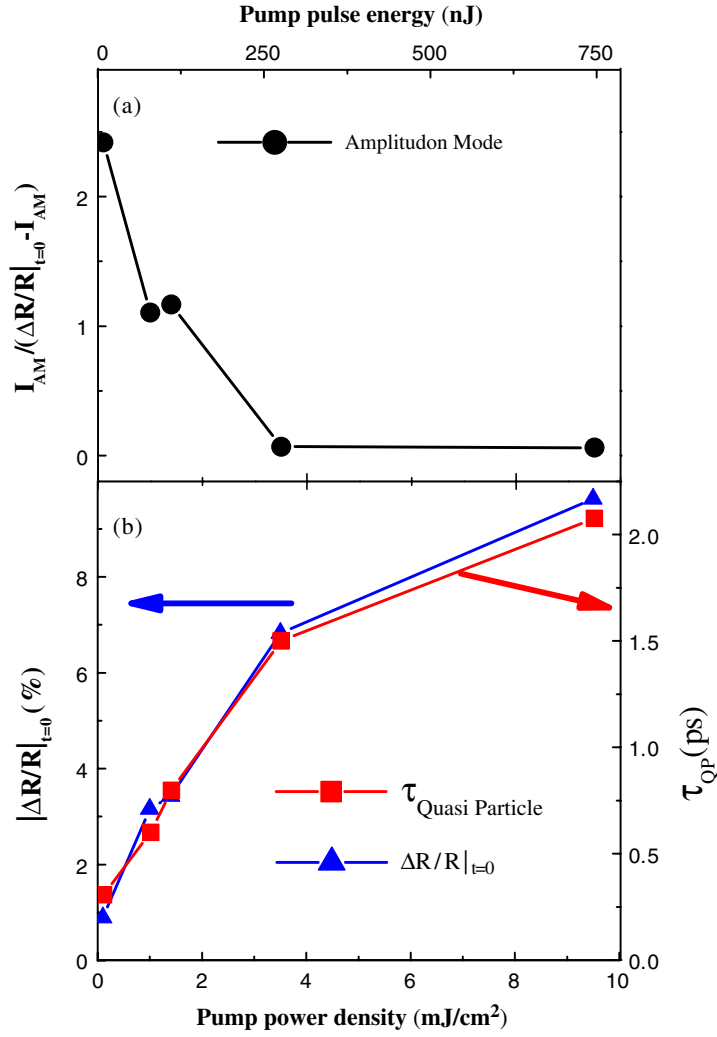


Figure 5. (a) Pump energy dependence of the ratio between the amplitudon, I_{AM} , and the quasi-particle response (the transient reflectivity at zero delay $\Delta R/R$, corrected for the amplitudon response). (b) Pump pulse energy dependence of the quasi-particle lifetime (τ) and amplitude of the quasi-particle peak ($\Delta R/R$). The quasi-particle lifetime and the quasi-particle peak show a linear increase with increasing pump pulse energy, while the AM amplitude shows a dramatic decrease. Experiments were performed at $T = 4.2$ K, using wavelengths 1150 and 800 nm for the pump and probe pulses, respectively. The solid lines are guides to the eye.

this special case, the dependence of the size of the coherent amplitudon response on $\Omega_{AM}\tau_{QP}$ is Lorentzian. This approach is reasonable as long as the quasi-particle response is slower than the temporal pump pulse width. For short quasi-particle relaxation times, the quasi-particle response becomes more symmetric, leading to a decaying exponential dependence of the coherent signal on $\Omega_{AM}\tau_{QP}$. To elucidate the point, figure 6 shows the amplitude of the coherent amplitudon response, normalized to the quasi-particle response, as a function of the coherence factor (symbols). The quasi-particle response is approximated as the product of its intensity and lifetime for a given pump pulse energy, which is sufficient for the present purpose.

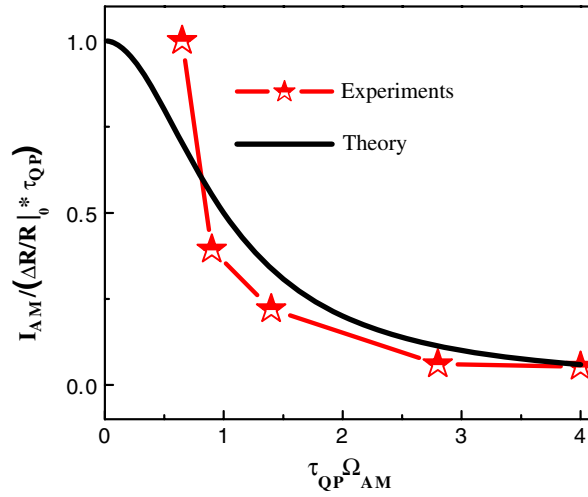


Figure 6. Normalized amplitude of the coherent AM as a function of the coherence factor $\tau_{QP}\Omega_{AM}$ (symbols). The decrease with increasing quasi-particle lifetime shows the loss of coherence due to the delayed relaxation of the quasi-particles. The solid line displays the amplitude of equation (2) as a function of the coherence factor.

Inspection of figure 6 shows that the intensity of the coherent amplitudon decreases rapidly as the coherence factor reaches unity, beyond which the coherence is lost due to the increase of the quasi-particle lifetime and hence dephasing of the generated amplitudons. The same figure also shows the amplitude obtained from equation (2), which given the crudeness of the model is in surprisingly good agreement with the data.

In addition to the decreasing size of the coherent response, the model proposed by (equation (2)) also predicts a phase shift of the coherent amplitudon response proportional to $\arctan(\Omega_{AM}\tau_{QP})$. The expected shift for the different τ_{QP} measured is small ($\sim\pi/10$), and not resolvable within the current experimental resolution. Moreover, this phase shift depends strongly on the shape of the quasi-particle excitation pulse, which experimentally shows a stretched exponential behaviour.

Some further evidence for the coupling of the photo-excited quasi-particles to the collective amplitudon mode of the charge density wave state may be found from the pump wavelength-dependent experiments discussed in the next section.

5. The wavelength dependence

Before discussing the pump wavelength-dependent transient CDW dynamics it is instructive to consider the linear optical response of the system. The linear optical response at various wavelengths provides information on possible absorption bands of the material, eventually giving more insight into the coupling of the electronic transitions with the CDW excitations.

Figure 7 shows the optical response in the wavelength region ranging from 270 to 1700 nm. The band observed in ϵ_2 below 500 nm is due to the ‘p-d’-transitions involving the electronic excitations from the oxygen ‘2p’ to the molybdenum ‘4d’ levels. The quotation marks are used to indicate that the levels are admixtures rather than pure ones. This is consistent with the photo-emission and electron energy loss experiments done on blue bronze [26, 27]. The broad asymmetric band around 1000 nm is due to interband ‘d-d’-transitions. The actual zero

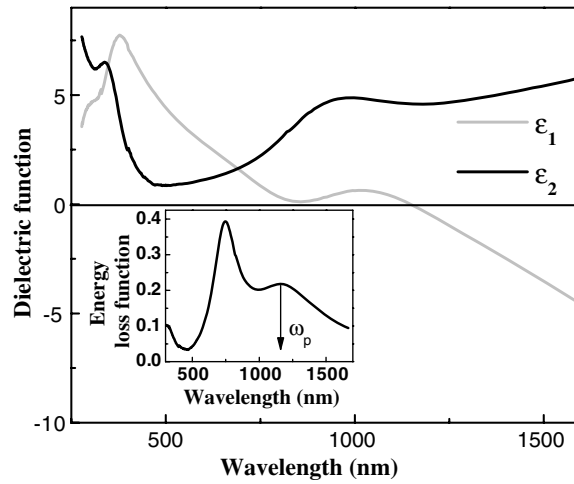


Figure 7. Optical response ϵ_1 and ϵ_2 of $K_{0.3}MoO_3$. Inset: the energy loss function calculated from the data in the main panel.

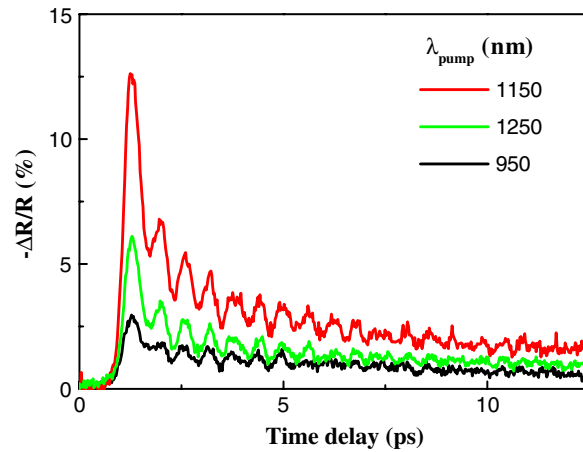


Figure 8. Variation of the transient response with the pump wavelength (pump energy 80 nJ/pulse, probe wavelength 800 nm).

crossing of ϵ_1 occurs at 1150 nm (1.08 eV). This, however, does not correspond to the actual plasma energy, which occurs at 1.5 eV [27]. This is also demonstrated in the inset of figure 7, which shows the energy loss spectrum calculated from the dielectric function. This spectrum shows two peaks, one at the actual plasma frequency (where also a distinct minimum in ϵ_1 is observed), and one at 1.08 eV. This latter energy corresponds to an interband plasmon involving the Mo-4d derived dispersionless conduction branch predicted by tight-binding calculations of Travaglini and Wachter [28, 27].

The transient response, and in particular the coherent amplitudon response, depends strongly on the excitation wavelength, and is found to be strongest for $\lambda_{\text{pump}} \sim 1150$ nm and at small wavelengths. This is demonstrated in figure 8, which shows the transient response for a few selected pump wavelengths (λ_{pump}).

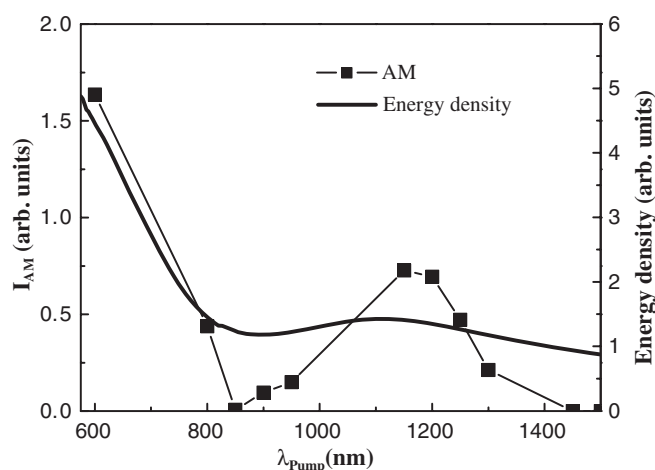


Figure 9. Coherent amplitudon response as a function of the pump wavelength (symbols; the line drawn is a guide to the eye). The absorbed energy density calculated from the optical constants in figure 7 (solid line).

Overall, the amplitude of the coherent amplitudon mode follows the pump energy absorbed in the material. This can be seen from figure 9, which shows the amplitude of the coherent amplitudon mode measured for various pump wavelengths at a constant pump energy of 80 nJ/pulse (1 mJ cm^{-2}). The same graph also shows the amount of absorbed pump energy density calculated from the optical data in figure 7. It is found that the quasi-particle lifetime does not vary strongly with the wavelength. This, together with the fact that the efficiency of the coherent amplitudon generation roughly follows the amount of absorbed energy, and hence the number of photo-excited quasi-particles, suggests once again the quasi-particle-induced nature of the coherent excitation.

Although the coherent AM roughly follows the absorbed energy curve, it does actually not exactly scale with it. In particular, the AM response (as well as the quasi-particle response) is markedly peaked near 1150 nm, corresponding to the interband plasma wavelength discussed above. This is surprising, since one does not expect the light to couple directly to the plasmon modes (as can also be seen from figure 7). Nevertheless, the experiments do evidence an efficient coupling, most likely through highly excited quasi-particles which relax by the emission of plasmon excitations, or through a coupling to surface plasmons. Once excited, the interband plasmons can relax either by emission of lower-energy quasi-particles which subsequently can excite amplitudons, as the enhanced quasi-particle response seems to suggest, or possibly even directly via decay into amplitudon modes.

6. Conclusion

In summary, we studied $\text{K}_{0.3}\text{MoO}_3$ using time-resolved spectroscopy, ellipsometry, and polarized Raman spectroscopy. The transient reflectivity experiments show, in addition to the coherent amplitudon mode observed previously [17], two coherent phonon modes which are also observed in the low-temperature Raman spectra. They are assigned to zone-folding modes associated with the charge density wave transition. The lifetime of the coherent amplitudon mode is found to be relatively short compared to the coherent phonons, which is believed to be due to the coupling of the AM to the high density of quasi-particles.

The generation of coherent amplitudon mechanism in blue bronze has been discussed. Whereas the quasi-particle generation is found to be proportional to the excitation energy (up to 300 nJ/pulse), the amplitude of the coherent amplitudon mode clearly lacks this proportionality. This makes it questionable whether DECP is indeed the generating mechanism for the observed coherent amplitudons. Based on the experimental observation that the size of the amplitudon response correlates with the coherence factor (i.e. with the inverse of the quasi-particle lifetime), a phenomenological model has been proposed here, in which the ultrafast decay of the photo excited quasi-particles is responsible for transferring the energy to the coherent excitation. One crucial aspect of this model is that the amplitudons generated by the quasi-particle decay process should have the same phase. Possibly bosonic amplification, in which the generated amplitudons phase lock to already generated amplitudons, plays a role here. Finally, the frequency-dependent experiments, where the transient reflectivity response is found to be consistent with the equilibrium absorption determined using ellipsometry measurements, are in line with the proposed generation mechanism. One surprise from the wavelength-dependent experiments is that the generation of coherent amplitudons and quasi-particles is strongly enhanced for wavelengths in the vicinity of the interband plasmon, suggesting an efficient coupling of the charge excitations to the interband plasmon excitations.

The mechanism proposed here could be a relevant generation mechanism of coherent excitations in other highly absorbing materials as well. Unfortunately, the weak coherent phonons observed in the present experiments do not allow for an analysis as has been done for the coherent amplitudon response. Further investigations, in particular concerning the phase lock of the amplitudon modes emitted in the quasi-particle decay process, and the observation of similar phenomena in other compounds are necessary to further develop the simple model proposed here.

Acknowledgments

This work was partially supported by the *Stichting voor Fundamenteel Onderzoek der Materie* (FOM, financially supported by the *Nederlandse Organisatie voor Wetenschappelijk Onderzoek* (NWO)).

References

- [1] Peierls R E 1930 *Ann. Phys., Lpz.* **4** 121
- [2] Peierls R E 1955 *Quantum Theory of Solids* (New York: Oxford University Press)
- [3] Grüner G 1988 *Rev. Mod. Phys.* **60** 1129
- [4] Grüner G 1994 *Density Waves in Solids* (Reading, MA: Addison-Wesley)
- [5] Wang F, Alvarez J V, Mo S-K, Allen J W, Gweon G-H, He J, Jin R, Mandrus D and Höchst H 2006 *Phys. Rev. Lett.* **96** 196403
- [6] Fleming R M and Grimes C C 1979 *Phys. Rev. Lett.* **42** 1423
- [7] Sirbu S, van Loosdrecht P H M, Yamauchi T and Ueda Y 2006 *Eur. J. Phys. B* **53** 289
- [8] Schlenker C and Dumas J 1986 *Crystal Chemistry and Properties of Materials with Quasi-One Dimensional Structures* ed J Rouxel (Dordrecht: Riedel)
- [9] Travaglini G and Watcher P 1981 *Solid State Commun.* **37** 599
- [10] Pouget J P, Kagoshima S, Schlenker C and Marcus J 1983 *Phys. Lett.* **L44** 113
- [11] Frölich H 1954 *Proc. R. Soc. A* **223** 296
- [12] Lee P A, Rice T M and Anderson P W 1974 *Solid State Commun.* **14** 703
- [13] Degiorgi L, Alavi B, Mihály G and Grüner G 1991 *Phys. Rev. B* **44** 7808
- [14] Escribe-Filippini C, Pouget J P, Hennion B and Sato M 1987 *Synth. Met.* **19** 931
- [15] Hennion B, Pouget J P and Sato M 1992 *Phys. Rev. Lett.* **68** 2374
- [16] van Loosdrecht P H M, Beschoten B, Dotsenko I and van Smaalen S 2002 *J. Physique IV* **12** 303

- [17] Demsar J, Biljakovic K and Mihailovic D 1999 *Phys. Rev. Lett.* **83** 800
- [18] Demsar J, Forró L, Berger H and Mihailovic D 2002 *Phys. Rev. B* **66** 041101
- [19] Mihailovic D, Dvoršek D, Kabanov V V, Demsar J, Forró L and Berger H 2002 *Appl. Phys. Lett.* **80** 871
- [20] Tsvetkov A A, Sagar D M, van Loosdrecht P H M, van der Marel D and van Smaalen S 2003 *Acta Phys. Pol. B* **34** 387
- [21] Zeiger H J, Vidal J, Cheng T K, Ippen E P, Dresselhaus G and Dresselhaus M S 1992 *Phys. Rev. B* **45** 768
- [22] Biljakovic K 1993 *Phase Transitions and Relaxations in Systems with Competing Energy Scales* ed T Riste and D Sherington (Dordrecht: Kluwer–Academic) p 339
- [23] Odin J, Lasjaunias J C, Biljakovic K, Hasselbach K and Monceau P 2001 *Eur. Phys. J. B* **24** 315
- [24] Staresinic D, Hosseini H, Brutting W, Biljakovic K, Riedel E and van Smaalen S 2004 *Phys. Rev. B* **69** 113102
- [25] Demsar J, Averitt R D, Taylor A J, Kabanov V V, Kang W N, Kim H J, Choi E M and Lee S I 2003 *Phys. Rev. Lett.* **91** 267002
- [26] Wertheim G K, Schneemeyer L F and Buchanan D N E 1985 *Phys. Rev. B* **32** 3568
- [27] Sing M, Grigoryan V G, Paasch G, Knupfer M, Fink J, Lommel B and Assmus W 1999 *Phys. Rev. B* **59** 5414
- [28] Travaglini G and Wachter P 1985 *Charge Density Waves in Solids (Springer Lecture Notes in Physics)* ed G Hutiray (Berlin: Springer) p 115